

# Sensory Monitoring of Drop Hammer Experiments with Multivariate Statistics

Matthias Muhr,<sup>[a]</sup> Thomas M. Klapötke,<sup>\*,[b]</sup> and Gerhard Holl<sup>[a]</sup>

**Abstract:** A precise characterization of substances is essential for the safe handling of explosives. One parameter regularly characterized is the impact sensitivity. This is typically determined using a drop hammer. However, the results can vary depending on the test method and even the operator, and it is not possible to distinguish the type of decomposition such as detonation and deflagration. This study monitors the reaction progress by constructing a drop hammer to measure the decomposition reaction of four different primary explosives (tetrazene, silver azide, lead azide, lead styphnate) in order to determine the reproducibility of this method. Additionally, further possible evaluation methods are explored to improve on the current binary statistical analysis. To determine whether classification was possible based on extracted features, the responses of

equipped sensor arrays, which measure and monitor the reactions, were studied and evaluated. Features were extracted from this data and were evaluated using multivariate methods such as principal component analysis (PCA) and linear discriminant analysis (LDA). The results indicate that although the measurements show substance specific trends, they also show a large scatter for each substance. By reducing the dimensions of the extracted features, different sample clusters can be represented and the calculated loadings allow significant parameters to be determined for classification. The results also suggest that differentiation of different reaction mechanisms is feasible. Testing of the regressor function shows reliable results considering the comparatively small amount of data.

**Keywords:** Explosives • sensor array • sensory characterisation • multivariate statistics • impact monitoring

## 1 Introduction

Performance and safety are important aspects of modern explosives [1]. In order to ensure safe handling of explosives and to prevent accidents, it is important to determine characteristic values for the sensitivity of these materials. The drop hammer test is one of the simplest and fastest methods for determining the impact sensitivity of energetic materials, which is a measure of the kinetic energy that must be applied to cause a material to combust [2,3]. In drop hammer tests, this value is determined by the kinetic energy of a drop weight dropping on a sample. A major disadvantage, however, is that such measurements cannot provide information about the type and violence of the reaction [4]. Other disadvantages include sample-to-sample variability and subjectivity of the operator [1,5–8]. In addition, different types of drop hammers are used in different laboratories, and therefore, the results can only be compared to a limited extent [1,4,9,10]. The initiation with drop hammer is poorly understood and not comparable to other initiation mechanisms [5,7,11].

The Bundesamt für Materialprüfung's (BAM) drop hammer is often used for the characterisation of explosives [12,13]. Klapötke et al. have found that results with the BAM drop hammer provide only limited results regarding the impact sensitivity. The reason for this is the sample preparation between two bolts in a cylinder, in which the

impact on the weight can ignite the sample by adiabatic compression [1]. An apparatus that compensates for this shortcoming is the OZM ball impact tester (BIT) [14]. With this device, sample is smoothed on a metal surface without damaging it, and a steel ball serves as a drop weight [14,15].

[a] M. Muhr, G. Holl  
Institut für Detektionstechnologien  
Hochschule Bonn-Rhein-Sieg  
von-Liebig-Str. 20  
53359 Rheinbach  
Deutschland  
\*e-mail: E-Mmmatthias.muhr@h-brs.de  
gerhard.holl@h-brs.de

[b] T. M. Klapötke  
Faculty for Chemistry and Pharmacy  
Ludwig-Maximilians Universität  
Butenandtstrasse 5–13  
81377 München  
Deutschland  
\*e-mail: Thomas.M.Klapoetke@cup.uni-muenchen.de

© 2022 The Authors. Propellants, Explosives, Pyrotechnics published by Wiley-VCH GmbH. This is an open access article under the terms of the Creative Commons Attribution Non-Commercial NoDerivs License, which permits use and distribution in any medium, provided the original work is properly cited, the use is non-commercial and no modifications or adaptations are made.

Other approaches to reduce the problems associated with using the drop hammer method have been explored in various publications, such as equipping drop hammers and other methods for initiating explosives with sensors [7,9,16–18]. An important example of these methods is the glass anvil drop hammer, which enables recordings of reaction processes using a high-speed camera. The use of the glass anvil drop hammer allows hotspots to be detected and measured. Likewise, processes such as phase transitions can be observed immediately before the ignition of the substance [4,19]. In addition, Klapötke et al. determined that individual substances emit different sound levels during combustion [2]. Reactions were examined spectroscopically and with pyrometers. These publications show that it is possible to detect different kinds of reactions in substances and for some substances even two successive reactions can be observed [6,20]. However, it is difficult to determine reproducible parameters for substances, since the reactions vary both in course and violence [6].

Various statistical methods such as  $E_{50}$ , no-fire-level, 1-out-of-10 etc. are used to evaluate drop hammer tests [2,12]. These methods are sufficient for the evaluation of the pure binary test response. However, the data resulting from sensory monitoring cannot be accurately and completely analysed with such methods. Nefati et al. have attempted to train neural networks with databases of impact sensitivities of explosives and predict their characteristics [21]. By applying multivariate statistics, it is possible to determine characteristic values and their correlations to the properties of explosives, which could improve on a purely binary evaluation [16,22]. Going further with this idea, we evaluate the possibility of visualisation of the multidimensional measurement results of drop hammer experiments to find clusters and correlations according to substance specific features.

In this publication, a drop hammer similar to the OZM BIT was constructed. It was equipped with a sensor array consisting of a pyrometer, a spectrometer, a VIS diode, a microphone and a piezo vibration sensor. This drop hammer was then used to measure tetrazene, silver azide, lead azide and lead styphnate, whereby the energy of the ball was adjusted so that all samples decomposed safely. The measured data was checked for the progression of the reactions and 42 features were extracted from each measurement. The extracted features were analysed using multivariate statistics. Clusters and substance specific features were extracted.

The aim of the measurements was to find out how reproducible the sensor reactions of the materials are. Additionally, it was investigated whether the substances can be distinguished based on the sensor responses and extracted features.

## 2 Experimental Section

### 2.1 Drop Hammer

A drop hammer was constructed based on the Ball Impact Tester (BIT) from the company OZM, since measurements with this apparatus, compared to the BAM drop hammer, provide more realistic results [1]. A steel ball is dropped onto a sample from a defined height in order to initiate combustion. Figure 1 shows the basic setup of the test stand, consisting of a stainless-steel base plate, which can be screwed to the table for stability (a), a head part, on which an electromagnet is installed with which the ball can be held or dropped (b), an aluminium rod, on which the head can be fixed continuously (c), and a ceramic plate, on which the sample is placed (d). In the BIT, the sample is applied to a steel plate. However, this shows wear in the form of depressions and corrosion after a few tests. Since these damages can varnish or interfere with measurements, a significantly harder  $Al_2O_3$  ceramic plate was used instead in this setup.

In the conventional BIT, the ball is released via a ramp with a flap, which causes the ball to rotate. This can cause friction, which initiates the sample in addition to impact [1]. The position at which the ball hits can also vary based on the height from which the ball is dropped. Thus, without camera monitoring, it is difficult to decide if a sample with a negative result was not hit, or if the initiation energy was

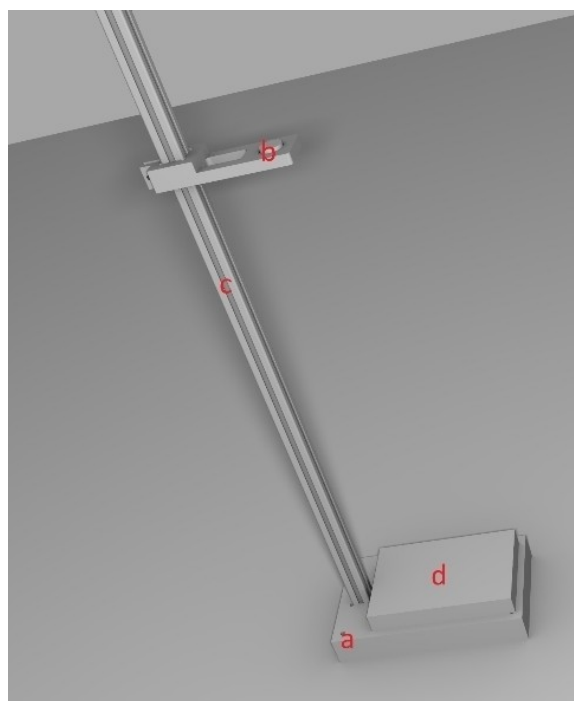


**Figure 1.** Model of the revised structure of the drop hammer - a: base plate, b: head plate with electromagnet, c: extrusion profile for height adjustment, d: ceramic plate for sample preparation.

not sufficient. To counteract this, an electromagnet was used in this setup, so that the ball always falls vertically. The height can be set between 5 cm and 95 cm by adjusting the position of the electromagnet on the rod. By using different steel balls (8.91 g–23.86 g), energies of 4.4 mJ to 222 mJ can be achieved.

## 2.2 Sensor Array

For the sensory monitoring of the setup, a sensor array consisting of various sensors was attached to the drop hammer. Figure 2 shows a schematic diagram of the sensor chamber of the drop hammer. The sensor array consists of a pyrometer (Kleiber Series 840(a)), a spectrometer (Ocean Optics USB 2000) with a 50  $\mu\text{m}$  fibre and a collimating lens (Ocean Optics 74-VIS Collimating Lens(b)), a photodiode (Conrad Electronic TRU COMPONENTS 1000 nm 3004 M1 C (c)), a MEMS microphone (ELV MEMS1 (d)) and a piezo shock sensor (TE Connectivity Vibration Sensor (e)). The sensor chamber is encapsulated in a housing (f) with openings for the ball (f1) and for the pyrometer (f2). For data acquisition (apart from the spectrometer, since it has a Serial COM port), a DAQ card (National Instruments, PCI-6122) was used for differential and simultaneous readout. The sampling rate was 100 kS/s and all sensors on the DAQ card were read out single ended. The spectrometer recorded one spectrum per measurement with an integration time of 100 ms.

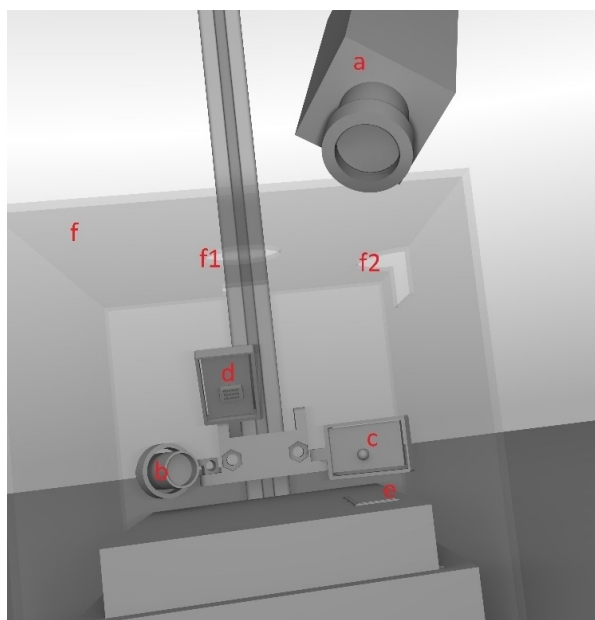


**Figure 2.** Sensor array of the drop hammer - a: pyrometer, b: spectrometer + collimator, c: VIS diode, d: MEMS microphone, e: piezo sensor, f: housing, f1: aperture for ball, f2: aperture for pyrometer.

## 2.3 Samples and Sample Preparation

Four different explosives were tested during the measurements: tetrazene ( $\text{C}_2\text{H}_6\text{N}_{10}$ , water content: 30%), silver azide ( $\text{AgN}_3$ , water content: 15%), lead azide ( $\text{Pb}(\text{N}_3)_2$ , water content: 30%) and lead styphnate ( $\text{C}_6\text{H}_9\text{N}_3\text{O}_8\text{Pb}$ , water content: 30%). All explosives were provided by DyniTEC GmbH. Sugar was also measured to determine the influence of the ball impact on the microphone and the piezo crystal, and to differentiate it from the signal of the explosive. In addition, blank measurements were made.

The sample preparation was standardised by first drying the sample in a desiccator for 12 hours, and subsequently placing it on the ceramic plate of the drop hammer according to the sample preparation used for the BIT [1]. As shown in Figure 3, the preparation involved a measuring spoon (a) being used to apply 10  $\mu\text{L}$  of the sample (b). The sample was then smoothed to a thickness of 0.3 mm with a slider and a rail (c, d).

The substances described above, and the corresponding sample preparation, were applied for all measurements.

## 2.4 Measurement Parameters

The drop hammer was set to a height of 50 cm. A 9.81 g ball was used, resulting in an energy of 48 mJ. This energy is higher than the impact sensitivity of the explosives used (tetrazene E16.6: 21 mJ, silver azide E16.6: 29 mJ, lead azide E16.6: 37 mJ, lead styphnate monohydrate: 2.5–5 J (all determined with BAM drop hammer) [4,5]). The parameters were left unchanged across all measurements. The samples were neither tilted nor were individual particle sizes sieved out. 20 measurements per substance were performed. With each attempt, all sensors were logged for three seconds. The data recording starts one second before the magnet is deactivated and the ball falls.

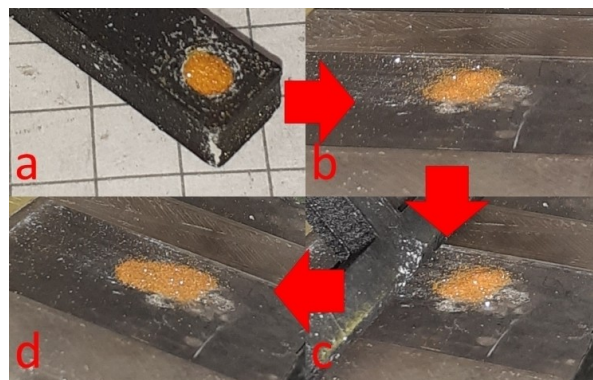


**Figure 3.** Sample preparation for the drop hammer test, a: measure the amount of substance, b: apply on the plate, c: smooth with slider, d: prepared sample with 0.3 mm thickness

## 2.5 Pre-Processing and Statistics

The sensor responses of the measurements were pre-processed and evaluated using a Python script [23]. The time axis of the sensors (excluding the spectrometer) was normalised to the first exceeding of a threshold value of the piezo signal. For all plots of the raw data, a section of 10 ms before and 100 ms after this peak was extracted from the signals recorded by all sensors. The piezo sensor was chosen because a specific change in the sensor signal can be expected even with blank substances. By adjusting the temporal offsets of the sensor, signals can be estimated and compared. A blank spectrum was performed immediately before the main measurement and subtracted as a background measurement from the spectrum.

To extract and display substance specific characteristics from the measurements, 42 features were extracted from each measurement. The integral of the entire emission spectrum and the wavelength with the maximum intensity were extracted from the spectrometer data. Ten features were extracted from each of the other sensors: the maximum of the signal, the signal integrated over time, the time of the maximum, the time at which the signal exceeds the threshold for the first time, the time at which the signal exceeds the threshold for the last time, the slope from the start of the peak to the maximum, the width of the peak, the width of the peak at half the height of the maximum, the width of the peak divided by the maximum of the peak and the width at which the signal exceeds the measurement range. The last feature describes the duration during which the signal is outside the measuring range.

Since the extracted 42 features had too many dimensions for a graphical evaluation, they were reduced using Principal Component Analysis (PCA). For this purpose, the data was first pre-processed using a unit vector and then calculated using scikit-learn's PCA library with standard parameters [24] to calculate three principal components. Through the reduced dimension it can be determined whether clusters become apparent when the data is plotted. The loadings can then be used to identify which of the extracted features could be useful for characterising and identifying the substances and which features are obsolete or redundant. The library scikit-learn [24] with singular value decomposition as the solver was also used to perform the LDA, using the entire dataset of extracted features. Since this method belongs to the supervised methods, it is not only possible to search for substance specific clusters in the data, but also to determine a regressor function. With the regressor function, identification of unknown samples is possible. Despite the relatively small data set, the correctness of the regressor function was determined by cross-validation, using the leave-one-out cross-validation procedure. In this process, each measurement is used iteratively over all measurements as test data set. The regressor function was calculated from the rest of the dataset and the average error rate of all measurements was calculated.

## 3 Results and Discussion

### 3.1 Sensor Data

In the following chapter, a characteristic measurement for each sensor is shown for all types of explosives.

#### 3.1.1 VIS Diode

The sensor responses of the VIS diode are shown in Figure 4. Sharp peaks can be seen in the sensor responses of lead styphnate, silver azide and lead azide, which are probably caused by a fast and violent decomposition of the sample [7,22]. Looking at the sensor response of lead styphnate, a second, smaller and broader peak can be seen. This behaviour is frequently observed with this sample and in a wide range of intensities (Figure 9). It is also occasionally observed in measurements with azides. This is possibly due to a moderate decomposition reaction, as described by Basset et al. [5], when the sample particles are whirled up by the ball. This will be verified in future measurements using a high-speed camera. In measurements with tetrazene, there is usually no signal above the noise level.

#### 3.1.2 Pyrometer

The signals of the pyrometer (Figure 5) are very similar to those of the VIS diode. Concerning lead styphnate, lead azide and silver azide, we also see comparatively high peaks, which are due to a fast and violent reaction of the sample [6,7,22]. It is noticeable that these signals take significantly more time to dissipate in comparison to those of the VIS diode. This could be explained by the vapours released during the reaction. These emit IR radiation and last longer than the emission of visible light. It can also be seen

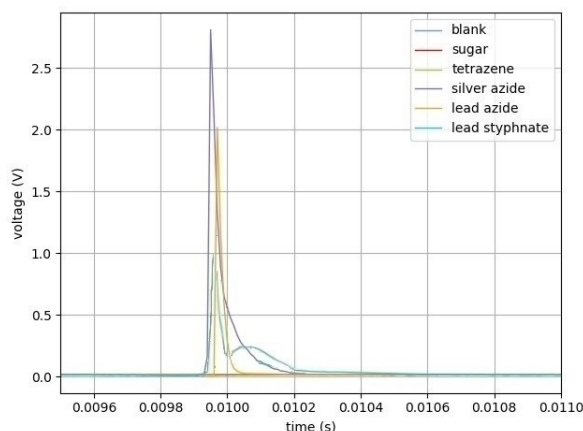


**Figure 4.** Characteristic signals of the VIS-diode of all six substances.

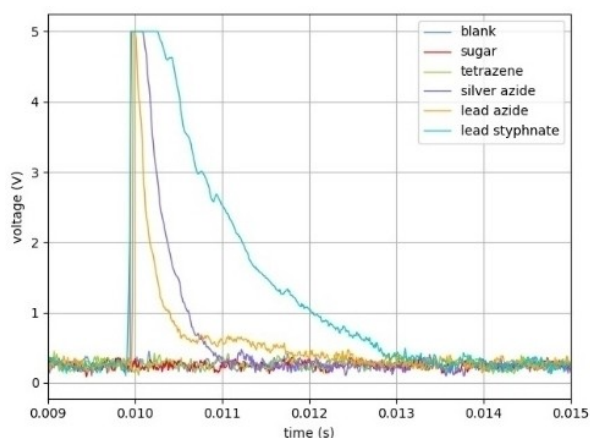


**Figure 5.** Characteristic signals of the pyrometer of all six substances.

that the signals are cut off at 5 V because the upper end of the measuring range of the Pyrometer has been reached. A second, smaller peak or tailing due to a mild side reaction is observed for the substances lead styphnate, lead azide and silver azide. As with the VIS diode, tetrazene does not produce any signal.

### 3.1.3 Microphone

Looking at the signals of the microphone (Figure 6), a signal can be detected in all samples. In the case of sugar and the blank measurement, this is generated exclusively by the impact of the ball. The signals are weakened when measured with sugar compared to the blank measurement, due to the fact that sugar mitigates the noise of impact compared to an impact between the steel ball and the ceramic plate. Signals of all explosives are clearly above those of the blank

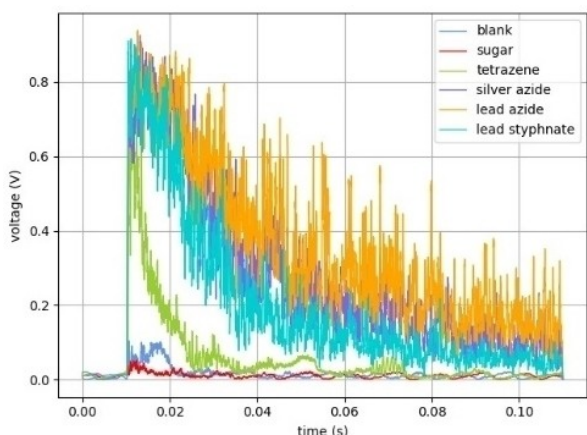


**Figure 6.** Characteristic signals of the microphone of all six substances.

substances. As with the pyrometer, it can be seen that the measuring range of the microphone is not sufficient. At an output voltage of about 0.9 V, the microphone membrane has reached its maximum amplitude. Comparing the width of the peaks, tetrazene shows the narrowest peaks. Measurements of lead azide and silver azide show similar sensor responses, while lead styphnate shows slightly shorter signals on average.

### 3.1.4 Piezo Sensor

Figure 7 shows the characteristic measurement signals of the piezo crystal. Looking at the measurements of the blank samples, a signal due to the ball is also recognisable. The signal of the explosives shows a similar behaviour for all types of explosives. First, a relatively high, sharp peak can be seen, followed by a chaotic oscillating decay. This is clearly less pronounced with tetrazene than with the other explosives investigated.

### 3.1.5 Spectrometer

The spectra of the measurements are shown in Figure 8. From each of the spectra shown, a blank measurement was taken immediately before the actual measurement. If one looks at the measurements of the blank substances, no peaks are recognisable. The same behaviour can be observed with tetrazene. Looking at the spectra of silver azide, peaks of the respective cations are visible (peaks silver: 256.423 nm, 466.847 nm, 519.817 nm, 546.549 nm, peaks lead: 405.780 nm, 589.562 nm, 500.541 nm, 256.423 nm [25]). However, since the wavelength is not considered in the evaluation, it is not discussed any further. Generally speaking, measurements of lead styphnate show a larger background than the spectra of the azides.

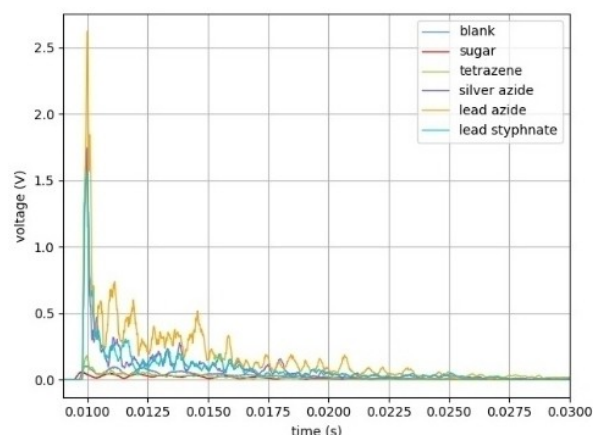


**Figure 7.** Characteristic signals of the piezo sensor of all six substances.

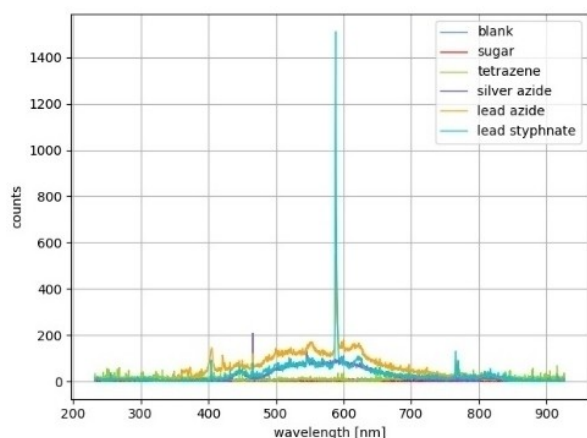


**Figure 8.** Characteristic signals of the spectrometer of all six substances.

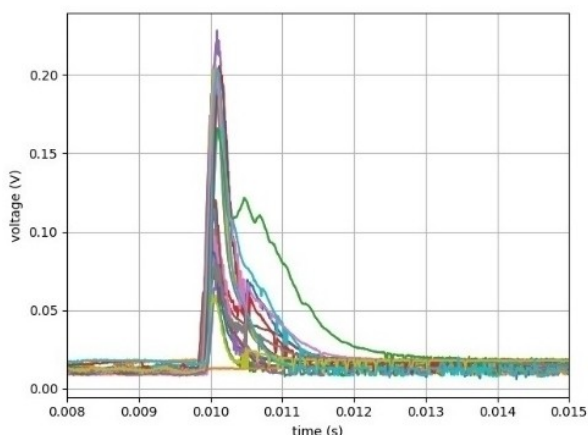


**Figure 9.** Lead styphnate - all 20 measurements, VIS-diode.

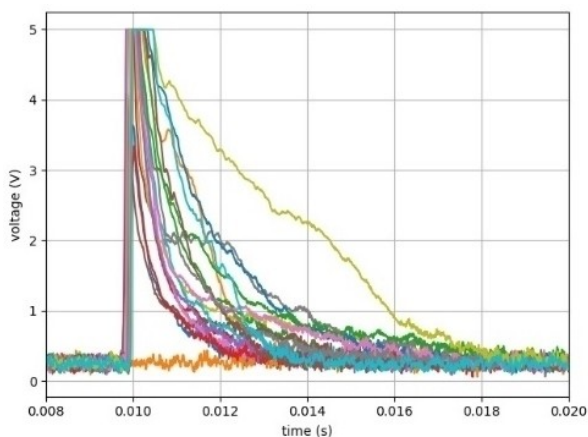


**Figure 10.** Lead styphnate - all 20 measurements, pyrometer.

### 3.2 Reproducibility of Lead Styphnate Measurements

If one compares the measurements from one sensor to another for an individual substance, it is noticeable that the sensor responses and signal curves are poorly reproducible. This applies to both the VIS diode and the pyrometer. Looking at the sensor responses of the VIS diode of lead styphnate (Figure 9), a main peak of the conversion can be identified in each measurement. As already described, this peak is narrow and highly pronounced. The intensity of this peak varies among all measurements. This main peak is sometimes followed by a second, smaller peak or tailing, which is caused by partial conversions of the particles dispersed through the ball. These reactions vary greatly in form and intensity.

The same behaviour can be observed in the signal curves of lead styphnate in the pyrometer (Figure 10). Here, all measurements show an initial high and comparatively narrow peak. It is noticeable that the end of the measuring range of the pyrometer is reached with almost every measurement, which makes an evaluation of the peak maximum difficult. The first peak is also partially followed by tailing caused by side reactions.

The measurement ranges of the VIS diode, the pyrometer and the microphone are problematic, since the signal of the sensors is cut off in many measurements. However, a reduction in sensitivity would have the disadvantage that substances that show comparatively mild reactions (e.g., tetrazene) could no longer be detected.

### 3.3 Feature Extraction and Discrimination

Features were extracted from the data of all measurements using the described Python script. All features were statistically evaluated and compared. Figure 11 shows the mean values of the integral of the pyrometer signals of all sub-

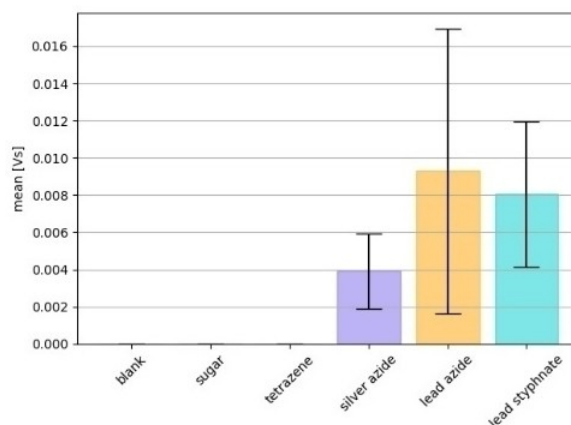


**Figure 11.** Average of the integral of the pyrometer signal, standard deviation drawn in.

stances. Silver azide, lead azide and lead styphnate clearly stand out from the blanks and tetrazene. Looking at the errors, it can be seen that the values of the extracted features scatter strongly. This correlates with the observations from Figure 10. As already described in the literature, the samples show a high scatter in the extracted features. Although trends can be seen in the mean values, the standard deviations are high. Based on the individual extracted characteristics, substance specific trends can be recognised, but a classification on the basis of this is not possible.

Looking at the pyrometer data (Figure 11), it is not possible to differentiate tetrazene from blank and sugar measurements. Lead azide, silver azide and lead styphnate differ significantly in their mean values, but the values are highly scattered. Looking at the average values of the integrated

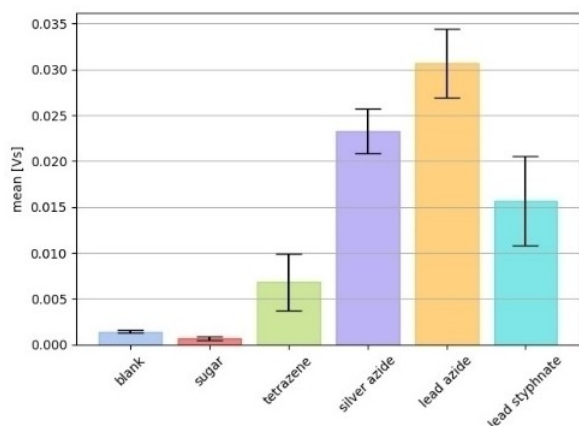


**Figure 12.** Average of the integral of the microphone, standard deviation drawn in.

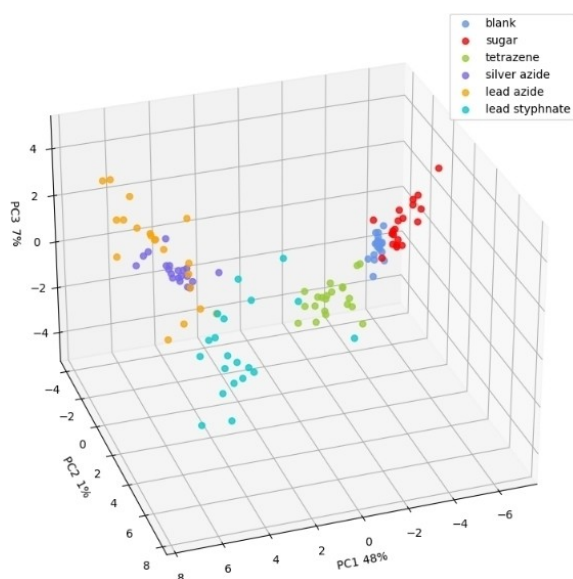


**Figure 13.** Plot of three calculated principal components.

microphone signals of all samples (Figure 12), clear gradations can be seen. It is possible to distinguish the substances based on this feature, but there is a high standard deviation.

The dimensions of the entirety of the extracted data are reduced to three dimensions using PCA. The variance of these dimensions is about 65%. Figure 13 plots the calculated three principal components against each other. The first principal component accounts for 48%, the second 10% and the third about 7% of the total variance of the data set. The substances tend to form clusters. Sugar and blank measurements consistently show negative values for PC 1. The measurements with tetrazene are comparatively close to the blank measurements. This is probably due to the mild combustion compared to the other explosives. Looking at the lead-containing compounds, they show a much stronger scatter than all other substances. Lead styphnate shows a very large expansion of the point cloud. This is consistent with the observations of high variances in the raw data and the extracted features.

Based on the results, it can be said that the substances are differentiable based on the reduced data set. Looking at the PCA loadings with the total variance of the individual sensors as a measure of separation (Figure 14), the signals from the VIS diode contribute most to the separation. The pyrometer, the microphone and the piezo crystal also contribute strongly to the separation and thus prove to be efficient for the differentiation of the measured substances. The weighting of the spectrometer is rather low. It can be omitted in future measurements.

Furthermore, the dimensions of the extracted features were reduced with an LDA. Figure 15 shows the reduced data set. The samples form clusters so that they can be distinguished based on the reduced data. As expected, the blank measurements show a relatively low dispersion. If we

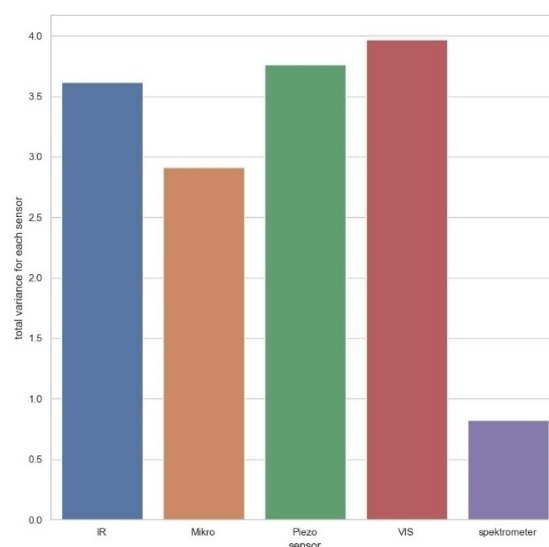


**Figure 14.** Total variance of each sensor.

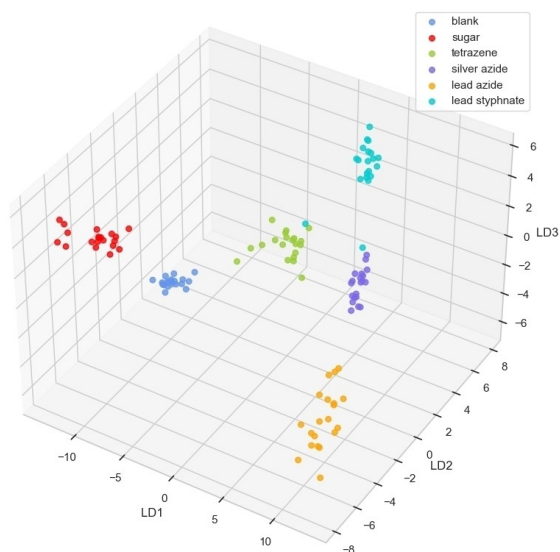


**Figure 15.** LDA of the extracted features.

look at tetrazene, all measurements are grouped, although highly scattered. Silver azide and lead azide also form clusters. Looking at lead styphnate, there are two outliers. Their cause and occurrence must be examined in more extensive measurement series. Lead styphnate tends to form clusters but the measurements scatter strongly. This is consistent with the observation that lead styphnate (Figure 9) gives very diverse sensor responses.

A regressor function was calculated and tested with a leave-one-out cross validation as described in chapter 2.5. The calculated error rate is 6.6%. Figure 16 shows the re-

blank	20	0	0	0	0	0
sugar	0	19	1	0	0	0
tetrazene	1	0	18	0	0	1
silver azide	1	0	0	19	0	0
lead azide	0	0	0	0	20	0
lead styphnate	1	0	1	2	0	16
	blank	sugar	tetrazene	silver azide	lead azide	lead styphnate

**Figure 16.** Confusion matrix of a leave-one-out cross validation.

sults of the cross validation in a confusion matrix. If we consider this, all blank measurements as well as all measurements with lead azide were correctly assigned. For sugar and silver azide, one measurement each was incorrectly assigned. For tetrazene, two measurements were incorrectly assigned, one as a blank measurement and the other as a lead styphnate measurement. This result also correlates with the observations. Two of lead styphnate measurements were assigned to silver azide and one each to the blank measurement and tetrazene. This is consistent with the occurrence of outliers in the data reduced by LDA.

The results are a preview for future measurements where the sample size will be significantly increased. The first results show the possibility of distinguishing between different substances, so that it may also be possible to distinguish between different decomposition mechanisms of the individual substances, such as detonation and deflagration.

## 4 Conclusion

A drop hammer was built in the style of the OZM BIT. The drop mechanism and the sample plates were changed. This setup was equipped with an array of different sensors: a microphone, a piezo vibration sensor, a VIS diode and a pyrometer. Four primary explosives, namely tetrazene, silver azide, lead azide and lead styphnate, were tested with this setup. The energy of the ball was selected so that all samples reacted adequately. The measurement data was first reviewed and the behaviour of the individual samples was analysed. It is noticeable that some substances show a high variance in sensor responses, especially lead styphnate. For some samples, the signals exceed the measuring range. It was not possible to counteract this issue, since other signals for substances such as tetrazene lie in the lower area of the measuring range. Thus, for future planned measurements, the dynamic range of the affected sensors will be expanded. In addition, several sensors with different measuring ranges will be used.

Features from all measurements were extracted and compared. Despite strong standard deviations of the individual features, substance specific trends are recognisable. Due to only small scatter in blank measurements, the influence of the setup on the total scatter of all samples is negligible. PCA was carried out for the purpose of dimension reduction. The substances tend to form clusters. When looking at the loadings, especially the signals of the VIS diode and the pyrometer contribute a large share to the total variance. The influence of the spectrometer on the total variance is rather small - for future measurements it can be omitted. To assess whether the extracted features are suitable for classification, an additional LDA was carried out, despite the comparatively small data set. The results of the LDA show that the substances cluster and a separation of

the substances could be possible by means of the extracted features.

Furthermore, the data show that it might be possible to identify different decomposition mechanisms of the substances and to depict parameters that favour the respective mechanisms. For future research, measurements with significantly higher sample sizes should be carried out to increase the precision of the regressor function. In addition, samples with different impact energies of the ball as well as different ball sizes are to be used to investigate the influence of these parameters on the decomposition of the samples.

## References

- [1] M. S. Gruhne, M. Lommel, M. H. H. Wurzenberger, N. Szimhardt, T. M. Klapötke, J. Stierstorfer, OZM Ball Drop Impact Tester (BIT-132) vs. BAM Standard Method – a Comparative Investigation, *Propellants Explos. Pyrotech.* **2020**, *45*, 147–153, <https://doi.org/10.1002/prep.201900286>.
- [2] T. M. Klapötke, Dropphammer Test Investigations on Some Inorganic and Organic Azides, *Propellants Explos. Pyrotech.* **2001**.
- [3] N. Lease, M. D. Holmes, M. A. Englert-Erickson, L. M. Kay, E. G. Francois, V. W. Manner, Analysis of Ignition Sites for the Explosives 3,3'-Diamino-4,4'-azoxyfurazan (DAAF) and 1,3,5,7-Tetranitro-1,3,5,7-tetrazoctane (HMX) Using Crush Gun Impact Testing, *ACS Mater. Au* **2021**, *1*, 116–129, <https://doi.org/10.1021/acsmaterialsau.1c00013>.
- [4] S. M. Walley, J. E. Field, R. A. Biers, W. G. Proud, D. M. Williamson, A. P. Jardine, The Use of Glass Anvils in Drop-Weight Studies of Energetic Materials, *Propellants Explos. Pyrotech.* **2015**, *40*, 351–365, <https://doi.org/10.1002/prep.201500043>.
- [5] Z. Men, W. P. Bassett, K. S. Suslick, D. D. Dlott, Drop hammer with high-speed thermal imaging, *Rev. Sci. Instrum.* **2018**, *89*, 115104, <https://doi.org/10.1063/1.5051357>.
- [6] Z. Men, K. S. Suslick, D. D. Dlott, Thermal Explosions of Polymer-Bonded Explosives with High Time and Space Resolution, *J. Phys. Chem. C* **2018**, *122*, 14289–14295, <https://doi.org/10.1021/acs.jpcc.8b02422>.
- [7] D. M. Williamson, S. Gymer, N. E. Taylor, S. M. Walley, A. P. Jardine, A. Glauser, S. French, S. Wortley, Characterisation of the impact response of energetic materials: observation of a low-level reaction in 2,6-diamino-3,5-dinitropyrazine-1-oxide (LLM-105), *RSC Adv.* **2016**, *6*, 27896–27900, <https://doi.org/10.1039/C6RA03096C>.
- [8] a) R. M. Doherty, D. S. Watt, Relationship Between RDX Properties and Sensitivity, *Propellants Explos. Pyrotech.* **2008**, *33*, 4–13, <https://doi.org/10.1002/prep.200800201>; b) M. J. Kamlet, H. G. Adolph, The relationship of Impact Sensitivity with Structure of Organic High Explosives. II. Polynitroaromatic explosives, *Propellants Explos. Pyrotech.* **1979**, *4*, 30–34, <https://doi.org/10.1002/prep.19790040204>.
- [9] C. S. Coffey, V. F. de Vost, Impact Testing of Explosives and Propellants, *Propellants Explos. Pyrotech.* **1995**, *20*, 105–115, <https://doi.org/10.1002/prep.19950200302>.
- [10] K. Thomas, *High Energy Materials*, Walter de Gruyter, Berlin, New York **2009**.
- [11] C. A. Handley, B. D. Lambourn, N. J. Whitworth, H. R. James, W. J. Belfield, Understanding the shock and detonation response of high explosives at the continuum and meso scales, *Applied Physics Reviews* **2018**, *5*, 11303, <https://doi.org/10.1063/1.5005997>.
- [12] J. Köhler, R. Meyer, A. Homburg, *Explosivstoffe*, 10. Auflage **2008**.
- [13] NATO standardization agreement (STANAG) 4489 Explosives, Impact Sensitivity Tests (4489) **1999**.
- [14] Ball-Drop Impact Tester BIT132, Ball-Drop Impact Tester BIT132 **2022**, <https://www.ozm.cz/sensitivity-and-explosibility-tests/ball-drop-impact-tester-bit132/>, accessed 11 August 2022.
- [15] United States Military Standard 1751 A (MIL-STD-1751 A), Safety and performance tests for qualification of explosives (high explosives, propellants and pyrotechnics), Method 1016, 2001 (MIL-STD-1751 A) **2001**.
- [16] S. Maurer, R. Makarow, J. Warmer, P. Kaul, Fast testing for explosive properties of mg-scale samples by thermal activation and classification by physical and chemical properties, *Sens. Actuators B* **2015**, *215*, 70–76, <https://doi.org/10.1016/j.snb.2015.03.045>.
- [17] J. G. Reynolds, P. C. Hsu, G. A. Hust, S. A. Strout, H. K. Springer, Hot Spot Formation in Mock Materials in Impact Sensitivity Testing by Drop Hammer, *Propellants Explos. Pyrotech.* **2017**, *42*, 1303–1308, <https://doi.org/10.1002/prep.201700115>.
- [18] P. J. Rae, P. M. Dickson, Some Observations About the Drop-weight Explosive Sensitivity Test, *J. dynamic behavior mater.* **2021**, *7*, 414–424, <https://doi.org/10.1007/s40870-020-00276-2>.
- [19] Y. Wu, H. Duan, K. Yang, H. Guo, F. Huang, Ignition and Combustion Developments of Granular Explosive (RDX/HMX) in Response to Mild-Impact Loading, *Propellants Explos. Pyrotech.* **2020**, *45*, 1250–1268, <https://doi.org/10.1002/prep.201900365>.
- [20] M. C. Phillips, B. E. Bernacki, S. S. Harilal, B. E. Brumfield, J. M. Schwallier, N. G. Glumac, Characterization of high-explosive detonations using broadband infrared external cavity quantum cascade laser absorption spectroscopy, *J. Appl. Phys.* **2019**, *126*, 93102.
- [21] H. Nefati, J.-M. Cense, J.-J. Legendre, Prediction of the Impact Sensitivity by Neural Networks, *J. Chem. Inf. Comput. Sci.* **1996**, *36*, 804–810, <https://doi.org/10.1021/ci950223m>.
- [22] K. Konstantynowski, G. Njio, G. Holl, Detection of explosives – Studies on thermal decomposition patterns of energetic materials by means of chemical and physical sensors, *Sens. Actuators B* **2017**, *246*, 278–285, <https://doi.org/10.1016/j.snb.2017.02.077>.
- [23] Python.org, Download Python **2021**, <https://www.python.org/downloads/>, accessed 14 September 2021.
- [24] scikit-learn, scikit-learn: machine learning in Python – scikit-learn 0.24.2 documentation **2021**, <https://scikit-learn.org/stable/>, accessed 19 August 2021.
- [25] NIST, Atomic Spectra Database **2020**, <https://www.nist.gov/pml/atomic-spectra-database>, accessed 14 September 2021.

Manuscript received: January 26, 2022  
Revised manuscript received: August 29, 2022